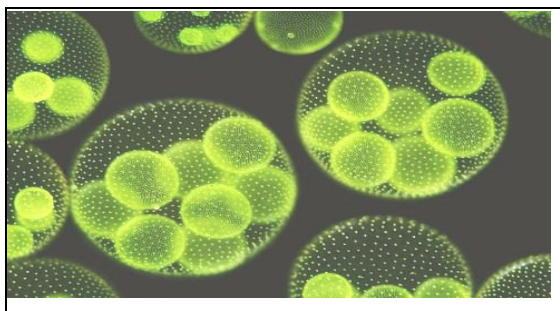

विज्ञान समाचार
SCIENCE NEWS

समाचार की तारीख : 8-12-2017
News date: 8/12/2017

संकल : डॉ अल्वारिनो लुईस
compiled by Dr. Alvarinho J. Luis

Algae could feed and fuel planet with aid of new high-tech tool

शैवाल (अलगे) नई उच्च तकनीक उपकरण की सहायता से ग्रह को खिला और ईंधन कर सकता है।

Vast quantities of medicines and renewable fuels could be produced by algae using a new gene-editing technique.

सारांश: एक नई जीन संपादन तकनीक का उपयोग करके शैवाल द्वारा बड़ी मात्रा-में दवाएं और अक्षय ईंधन का उत्पादन किया जा सकता है।

Scientists have devised a method that could lead to cheap, environmentally friendly ways of making products for use in the cosmetics, plastics and food industries.

Algae are highly prized for their ability to make useful products, but a lack of engineering tools has hindered basic research and growth of the industry for decades, researchers say.

Scientists at the University of Edinburgh sought to improve the efficiency of gene-editing to increase yields of products currently made using algae, including some food supplements. The advance could also enable algae to make new products, such as medicines.

The technique uses molecules that act like scissors to cut DNA -- called CRISPR molecules -- which allow researchers to add new genes or modify existing ones. Until now, scientists have struggled to develop a technique that works efficiently in algae.

To overcome this, the team added CRISPR molecular scissors and short pieces of DNA directly to algae cells to make precise modifications to the genetic code.

Their new method is more specific and increases efficiency 500-fold compared to previous techniques. The discovery could unleash the potential of the global algae industry, projected to be worth $1.1billion by 2024.

The team developed its technique to work in a widely used species of algae -- called Chlamydomonas reinhardtii. The method could potentially also be used to engineer crops to increase yields, improve disease resistance or enable plants to thrive in harsh climates.

The study, published in the journal *PNAS*, was funded by the Biotechnology and Biological Sciences Research Council and Scottish Bioenergy.

Dr Attila Molnar, of the University of Edinburgh's School of Biological Sciences, who led the study, said: Our findings mark a key advance in large-scale algal genome engineering. Our technique is applicable to a wide range of species, and could pave the way for the development of designer algae, which has many biotechnology applications.

Journal Reference:

Aron Ferenczi, Douglas Euan Pyott, Andromachi Xipnitou, Attila Molnar. Efficient targeted DNA editing and replacement inChlamydomonas reinhardtiiusing Cpf1 ribonucleoproteins and single-stranded DNA**. *Proceedings of the National Academy of Sciences*, 2017; 201710597 DOI: 10.1073/pnas.1710597114** **(pdf reprint follows)**

Efficient targeted DNA editing and replacement in *Chlamydomonas reinhardtii* using Cpf1 ribonucleoproteins and single-stranded DNA

Aron Ferenczi[a], Douglas Euan Pyott[a], Andromachi Xipnitou[a], and Attila Molnar[a,1]

[a]Institute of Molecular Plant Sciences, University of Edinburgh, Edinburgh EH9 3BF, United Kingdom

Edited by Sabeeha S. Merchant, University of California, Los Angeles, CA, and approved November 3, 2017 (received for review June 12, 2017)

The green alga *Chlamydomonas reinhardtii* is an invaluable reference organism to research fields including algal, plant, and ciliary biology. Accordingly, decades-long standing inefficiencies in targeted nuclear gene editing broadly hinder *Chlamydomonas* research. Here we report that single-step codelivery of CRISPR/Cpf1 ribonucleoproteins with single-stranded DNA repair templates results in precise and targeted DNA replacement with as much as ∼10% efficiency in *C. reinhardtii*. We demonstrate its use in transgene- and selection-free generation of sequence-specific mutations and epitope tagging at an endogenous locus. As the direct delivery of gene-editing reagents bypasses the use of transgenes, this method is potentially applicable to a wider range of species without the need to develop methods for stable transformation.

Chlamydomonas reinhardtii | CRISPR/Cpf1 | RNP | ssODN | editing

The model green microalga *Chlamydomonas reinhardtii* is an invaluable model organism at the interface of algal, plant, and ciliary biology (1, 2). For decades, *C. reinhardtii* has fueled research on photosynthetic gene function (3), and is an indispensable reference for studying the carbon concentrating mechanism (4, 5), ciliary function and composition (6–8), lipid metabolism and prospects of biofuel production (9–11), carotenoid biosynthesis (12) and nutrient starvation responses (13–15). *C. reinhardtii* is remarkably tractable as a result of its short generation time (8–10 h), haploid genotype, sequenced genome (16, 17), simple transformation methods (18–21), and plethora of resources, including the Chlamydomonas Resource Center (University of Minnesota) and *Chlamydomonas Sourcebook* (22).

Despite its auspicious features, nuclear gene targeting in *C. reinhardtii* through homologous recombination (HR)-mediated plasmid integration occurs at prohibitively low levels (18, 19, 23–28). This necessitates the positive selection of mutants through cointegration of antibiotic resistance markers. The recent use of single-stranded oligodeoxynucleotides (ssODNs) has reduced nontarget integration, but has left gene targeting extremely inefficient (29–32). Previous efforts to use targeting endonucleases, including zinc finger nucleases and Clustered Regularly Interspaced Short Palindromic Repeat (CRISPR)-associated protein 9 (Cas9), have not resolved these shortcomings in gene targeting efficiency (33–36).

RNA-programmable CRISPR endonucleases induce targeted dsDNA breaks, triggering cellular DNA repair pathways. Of these pathways, nonhomologous end-joining (NHEJ) results in random insertions and deletions (i.e., indels) at the target site (37, 38), whereas HR allows homology-directed, precise editing by using DNA repair templates. NHEJ-mediated gene editing efficiencies in *C. reinhardtii* using Cas9 are low, ranging from 10^{-8} to 1% (35, 36), and therefore require phenotype-based selection of mutants. In addition, CRISPR-mediated editing in *C. reinhardtii* is presently limited to NHEJ-mediated indel formation as a result of an apparent insufficiency in the nuclear HR pathway to carry out homology-mediated editing (35, 36).

Here, we report that transgene-free transfection into *C. reinhardtii* of preassembled CRISPR/Cpf1 ribonucleoproteins (RNPs), an ortholog of Cas9, can induce NHEJ-mediated indels with 0.02% efficiency, broadly matching Cas9 (32, 36). More importantly, cotransfection of Cpf1 RNPs with ssODNs acting as DNA repair templates results in precise, targeted DNA replacement at frequencies as high as 10%. This enables phenotype-independent identification of mutants edited with nucleotide-level precision at nuclear loci predisposed to Cpf1-mediated cleavage.

Results

Our goal was to devise an efficient Cpf1-mediated genome-editing platform for *C. reinhardtii*, a member of a basally diverged clade (*Chlorophyta*) of the plant kingdom (39). We first tested the activity of two Cpf1 orthologs in planta by *Agrobacterium*-mediated transient expression in *Nicotiana benthamiana*. As Cas9 activity in planta is correlated with activity in mammalian cells (40), we assayed the activity of *Acidaminococcus* Cpf1 (AsCpf1) and *Lachnospiraceae* Cpf1 (LbCpf1), the then known most active Cpf1 orthologs in mammalian cells (41, 42). By expressing AsCpf1, LbCpf1, Cas9, and corresponding guide RNAs (gRNAs) in *N. benthamiana*, we found the activity of LbCpf1 broadly matched Cas9, whereas AsCpf1 activity was barely detectable through a T7 cleavage assay (Fig. 1*A*). We concluded that LbCpf1 is more active than AsCpf1 in planta, in agreement with other recent studies (43–46), and therefore proceeded with LbCpf1 to edit *C. reinhardtii*.

To monitor LbCpf1-mediated genome editing in *C. reinhardtii*, we targeted *FK506-binding protein 12* (*FKB12*; Cre13.g586300) for knockout (KO). FKB12 mediates the interaction between the antibiotic rapamycin and the cell cycle regulator Target of Rapamycin, which leads to cell death. Consequently, *FKB12* loss-of-function

Significance

Our findings establish a method of efficient, targeted genome editing in *Chlamydomonas reinhardtii*. We demonstrate an approach to bypass inefficient gene targeting via homologous recombination and achieve homology-directed DNA replacement in *C. reinhardtii*. In addition, we report CRISPR/Cpf1-mediated DNA editing efficiencies being boosted 500-fold through the use of single-stranded oligodeoxynucleotides (ssODNs) as repair templates. It remains to be determined whether Cpf1-induced staggered DNA cleavage enhances ssODN-mediated gene editing in a wider range of species and whether the underlying repair pathway(s) responsible is more broadly conserved.

Author contributions: A.F. and A.M. designed research; A.F., D.E.P., A.X., and A.M. performed research; A.F. and A.M. analyzed data; and A.F. and A.M. wrote the paper.

Conflict of interest statement: A.M. and A.F. are coinventors on a patent application related to this work.

This article is a PNAS Direct Submission.

[1]To whom correspondence should be addressed. Email: attila.molnar@ed.ac.uk.

This article contains supporting information online at www.pnas.org/lookup/suppl/doi:10.1073/pnas.1710597114/-/DCSupplemental.

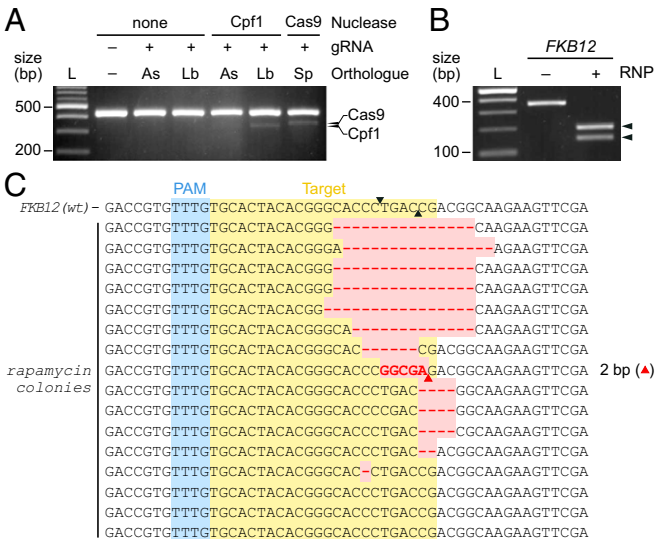

Fig. 1. Cpf1 activity in planta, in vitro, and in *C. reinhardtii*. (*A*) CRISPR nuclease orthologs *Acidaminococcus* sp. Cpf1 (AsCpf1), *Lachnospiraceae bacterium* Cpf1 (LbCpf1), and *Streptococcus pyogenes* Cas9 (SpCas9) were expressed in planta with corresponding gRNAs targeting the GFP locus in *Nicotiana benthamiana* line 16c. T7 mismatch endonuclease digestion of the PCR-amplified *GFP* locus from a mixed-population of cells results in cleaved products (black arrows), corresponding to edited DNA. L, ladder. (*B*) In vitro cleavage of PCR-amplified *FKB12* using LbCpf1 and gRNA RNPs. Arrowheads indicate cleaved products. L, ladder. (*C*) Sequencing of cells edited at *FKB12* using LbCpf1 RNPs. *FKB12* was amplified from rapamycin-resistant colonies growing on solid growth media with 10 μM rapamycin ($n = 16$). Black triangles indicate the expected LbCpf1-mediated cleavage site, red triangles indicate insertion sites with insertion lengths shown to the right of the sequence, and red highlighting indicates sequence deviation from the WT sequence (*Top*).

mutation results in high rapamycin tolerance (i.e., resistance), making it a suitable marker for positive selection in targeted mutagenesis (34, 47). We identified two LbCpf1 gRNA protospacer adjacent motifs (5′-TTTN-3′) within the second exon of *FKB12* and designed a gRNA for the one with no predicted off-target sites with Cas-OFFinder (48). We generated the gRNA by in vitro transcription and purified recombinant LbCpf1 protein from *Escherichia coli*. To assess the activity of our CRISPR reagents, the target *FKB12* locus was PCR-amplified and incubated with preassembled LbCpf1 and gRNA RNP complexes in vitro. The complete in vitro cleavage of the target locus confirmed active RNP formation (Fig. 1*B*).

To test the efficacy of LbCpf1 in vivo, we delivered the *FKB12*-targeting RNPs into *C. reinhardtii* cells (cc-1883; *cw15*) via electroporation and spread cells onto solid growth media containing 10 μM rapamycin (36). Cell viability, required to determine the proportion of rapamycin-resistant cells, was estimated from serial dilution of cells that had undergone identical electroporation treatment but without gRNA and were grown on media containing no rapamycin (Fig. S1).

Delivery of RNPs produced ∼0.02% rapamycin-resistant cells (Fig. S1). Through sequencing, we confirmed 13 of 16 rapamycin-resistant colonies having mutations at the LbCpf1 cut site (Fig. 1*C*), equivalent to a mutagenesis efficiency of 0.016%. This underrepresents total mutagenesis efficiency, as it only represented loss-of-function mutations. Colonies with no detectable *FKB12* mutations were most likely cells that escaped selection, as we never experienced total elimination of background cell growth even with the use of 20 μM rapamycin.

We next explored whether targeted DNA cleavage could be used to facilitate homology-mediated mutagenesis by using DNA repair templates. We employed ssODN templates, which reportedly provide 100-fold lower levels of nonhomologous integrations compared with double-stranded counterparts (29). Our ssODN was 118 nt long, designed with homology arms extending 49 and 45 nt upstream and downstream of the gRNA target site, respectively. It harbored replacement of the target site with a foreign sequence of equal length with stop codons inserted in all three reading frames. We tested the single-step codelivery of RNPs together with ssODNs in the sense or antisense orientation (Fig. 2*A*). To calculate editing efficiency, cells were serially diluted, and each dilution was plated onto solid growth media with and without rapamycin to estimate numbers of mutant cells and viable cells, respectively. Surprisingly, codelivery of RNPs and ssODN led to 22% and 18% rapamycin-resistant cells with the use of sense and antisense ssODNs, respectively (Fig. 2*B*). Sequencing of rapamycin-resistant colonies confirmed template integration in most cases ($n = 27$ of 32), although single-nucleotide indels and substitutions were scattered across the region of ssODN homology in half of all sequenced mutants ($n = 14$ of 27; Fig. 2*C* and Figs. S2 and S3). Two integration events resulted in duplication of the homology arms (Fig. S7). Importantly, scarless integration events represented 40% ($n = 13$ of 32) and 46% ($n = 6$ of 13) of rapamycin-resistant cells with the use of sense and antisense ssODNs, respectively, which we regarded as being broadly equivalent. As a proportion of viable cells, scarless, homology-mediated editing was achieved at 8–9% efficiency, which represents a ∼500-fold increase over non–ssODN-mediated KOs with the use of RNPs alone. In control experiments that used sense ssODNs without RNPs, resistant cells were rare (2×10^{-3}%; Fig. 2*B*), on par with previously established protocols (29, 31).

To demonstrate the utility of ssODN-mediated gene editing in *Chlamydomonas*, we epitope-tagged the endogenous *FKB12* in frame (Fig. 3*A*). We designed a sense ssODN as described here earlier and replaced the gRNA target site with six tandem histidine codons followed by an in-frame-stop codon. The stop codon allowed mutation efficiencies to be estimated from the frequency of rapamycin-resistant cells as before (Fig. 2*B*). Codelivery of RNPs and this ssODN yielded 29% rapamycin-resistant colonies (Fig. 3*B*). Sequences from six such colonies suggested that approximately half carried scarless integrations (Fig. 3*C*). This high frequency (>10% of viable cells) raised the possibility of identifying colonies containing scarless DNA replacement without first selecting against WT cells. This approach could be used even when the phenotypic effects of a mutation might not be obvious or are unknown. To test this, 13 randomly chosen colonies growing on nonselective medium (without rapamycin) were sequenced. One of these colonies carried the desired DNA replacement (representing 7% of viable cells), demonstrating viable selection- and phenotype-free identification of edited cells (Fig. 3*D*). Immunoblot analysis confirmed a detectable his-tagged protein of the expected size in the identified mutants (Fig. 3*E*), and is one of the first demonstrations of epitope tagging at an endogenous locus in *C. reinhardtii* (32).

To transfer our method into a cell-walled strain of *C. reinhardtii*, we attempted to edit *FKB12* in cell-walled strain cc-2931. The same electroporation conditions did not result in rapamycin resistance, even after treating cells with Maxx Efficiency Transformation Reagent (Fig. S4).

To explore the efficacy of LbCpf1 and ssODN-mediated editing at other nuclear loci, we targeted three additional genes in strain cc-1883: *CpFTSY* (Cre05.g241450), *CpSRP43* (Cre04.g231026), and *PHT7* (Cre16.g663600). CpFTSY and CpSRP43 are nuclear-encoded components of the chloroplast signal recognition particle and are involved in assembly of the chlorophyll light-harvesting complexes, also called antennae (49). Loss-of-function mutation at these loci results in truncated chlorophyll antennae, leading to lower chlorophyll content and hence a bright-green phenotype (36, 49, 50). Phenotypic screening for bright-green colonies therefore allows determination of loss-of-function mutation efficiency. In contrast, PHT7 is a putative

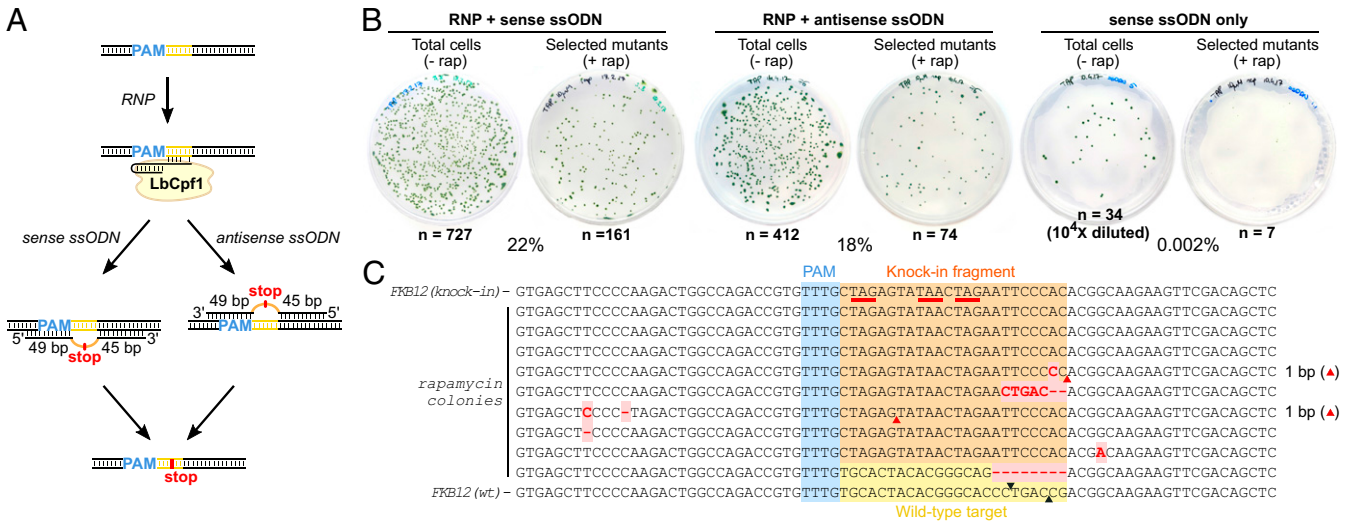

Fig. 2. Codelivery of RNPs and ssODNs into *C. reinhardtii*. (*A*) Schematic of sense or antisense ssODN-mediated DNA repair upon codelivery of RNPs and ssODNs. (*B*) Cells cotransfected with RNPs and sense or antisense ssODNs were serially diluted, and each dilution was spread onto solid growth media with and without rapamycin (rap, 10 μM). A dilution with countable numbers of colonies ("n") is shown for each treatment, and the percentage of rapamycin-resistant colonies is indicated. (*C*) Representative sequences of rapamycin-resistant colonies from the "RNP + sense ssODN" experiment. All sequence deviations from the expected knock-in (*Top*) and WT sequences (*Bottom*) within the span of the ssODN homology region are shown. Sequence highlighting is as in Fig. 1C. Stop codons are underlined in red. Sequences from all sequenced rapamycin-resistant colonies are collated in Figs. S2 and S3.

phosphate transporter in *C. reinhardtii* and was included to represent a locus with no known phenotype.

Interestingly, in vitro cleavage of *CpFTSY*, *CpSRP43*, and *PHT7* occurred with varying efficacies (Fig. 4*A*). Editing at these loci was performed by using ssODNs harboring the same target site replacement as before with in-frame stop codons. As expected, colonies with *CpFTSY* and *CpSRP43* mutations displayed a bright-green phenotype (Fig. 4*B* and Fig. S6). Surprisingly, *PHT7* mutants elicited a growth disadvantage and could be identified through a small-colony phenotype (Fig. 4*B* and Fig. S5*A*). Targeted editing at *PHT7* was therefore equally suitable for efficiency determination.

Targeted KO of *CpFTSY*, *CpSRP43*, and *PHT7* occurred in 0.5–16% of cells, of which ssODN-mediated, scarless DNA editing occurred in 0.1–8% of cells (Fig. 4 *C* and *D* and Figs. S5 and S6). Larger insertions were consistently a result of sequence duplications (Fig. S7). Together with editing at *FKB12*, ssODN-mediated, scarless targeted editing occurs with 0.1–10% efficiency, with overall KO efficiencies at a slightly higher 0.5–16%.

Discussion

Our work demonstrates that the use of CRISPR/LbCpf1 RNPs and ssODNs as DNA repair templates can perform efficient, homology-directed editing in *C. reinhardtii*. At four nuclear loci, we show scarless editing to occur with efficiencies of 0.1–10%, whereas scarred editing occurs with a frequency as high as 16%.

Nuclear homologous sequence replacement in *C. reinhardtii* has been reported as inefficient, which has been taken as evidence of low activity of the nuclear HR repair pathway (27). Our findings of gene-targeting efficiencies being much higher than previously reported suggests that an alternative homology-directed mechanism distinct from HR is invoked through ssODN-mediated repair. This might also be more broadly conserved within plants and eukaryotes. Indeed, in human cells, ssODN-mediated repair has been shown to be independent of canonical HR components BRCA2 and RAD51 (51, 52). In addition, the staggered cuts produced by Cpf1 may efficiently predispose to homology-mediated ligation of ssODNs at the cut site, potentially more so than at Cas9-mediated blunt cuts. Furthermore, high-throughput nuclear transgenesis of *C. reinhardtii* suggests that endonucleases extensively fragment transgenes before integration (53). This compounds the difficulties in performing precise, HR-mediated nuclear gene targeting. Use of ssODNs may bypass endonuclease recognition, although local ssODN fragment duplications still occur, presumably through stochasticity of the thermodynamic DNA annealing process (Fig. S7).

Despite the ∼500-fold enhancement of editing through supplementation of RNPs with ssODNs, we observed variability of two orders of magnitude in nuclear editing efficiencies at the four nuclear loci tested. These results partly reflect a lack of tools to predict Cpf1-mediated DNA cleavage efficiency (54), which are more abundant for Cas9 (55–59). In vivo Cpf1 cleavage efficiencies are distinct from Cas9 and markedly vary even within tens of bases of DNA (36, 60), which suggests a significant sequence-specific component to cleavage efficiency. We therefore take the lower range of our demonstrated editing efficiencies (0.1–1%) to reflect inefficient gRNA design. Curiously, DNA cleavage in vitro did not correlate with results in vivo (Fig. 4 *A* and *D*). This counterintuitive finding suggests to us that in vitro cleavage is not suitable to infer in vivo results. To increase editing efficiencies, lowering the number of electroporated cells, lowering the volume of electroporated cells, and increasing Cpf1 concentration might be employed. In addition, testing multiple targets per locus can empirically reveal efficient gRNAs (36, 57). We also conclude that editing of cell-walled *C. reinhardtii* strains will continue to require autolysin treatment to degrade cell walls before transfection (19). Pulsed, square-wave electroporation has also been optimized for cell-walled strains and may offer viable means of RNP transfection (32, 61).

Delivery of RNPs bypasses the need to develop a system for genetic transformation of the target species, including transgene optimization and selection of transgenic cells. The high potential efficiency of editing may also remove the need to select for mutants by phenotype. The approach could therefore be applicable to a wider range of green algal species, promoting their use in industry and basic research.

Materials and Methods

Generation of Cpf1, Cas9, and GFP-Targeting gRNA Constructs. Plasmid vectors containing human-codon optimized Cpf1 from *Acidaminococcus* sp. BV3L6 (AsCpf1) and *Lachnospiraceae* bacterium ND2006 (LbCpf1) were a gift from Feng Zhang, Broad Institute of MIT and Harvard, Cambridge, MA and McGovern

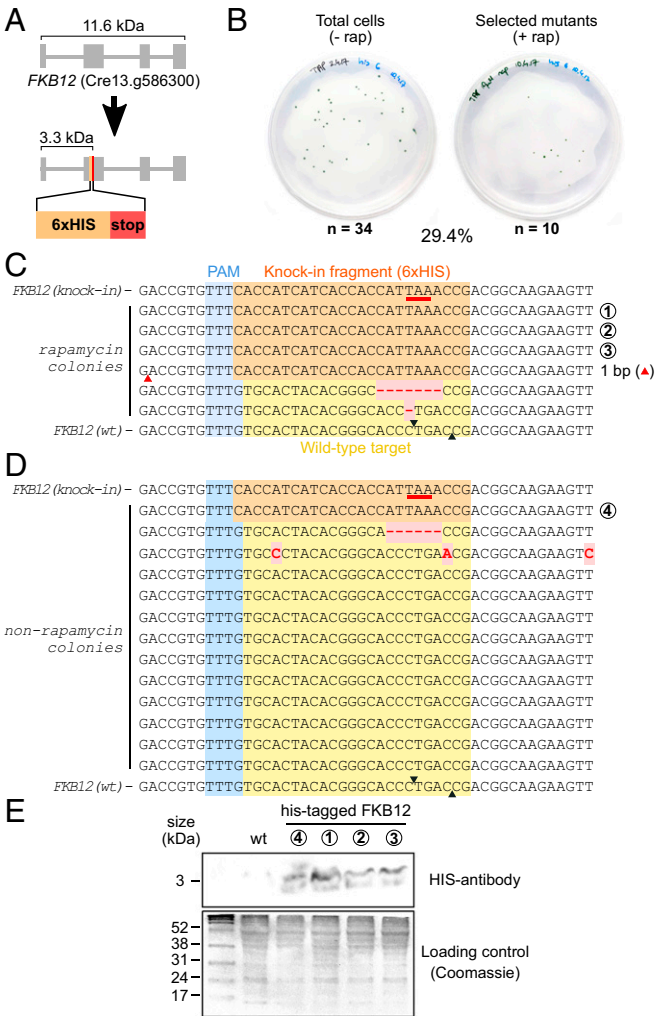

Fig. 3. Selection-free identification of his-tagged *FKB12* mutants. (*A*) Schematic of the his-tagged *FKB12* locus obtained using sense ssODNs carrying an in-frame 6xHIS-tag followed by a stop codon. (*B*) Cells cotransfected with RNPs and ssODNs are plated as described in Fig. 2*B*. (*C*) *FKB12* sequences of six rapamycin-resistant colonies from the plate with rapamycin shown in *B*, three of which carry scarless, ssODN-mediated editing. (*D*) *FKB12* sequences from 13 colonies randomly chosen from the plate without rapamycin in *B*, one of which carries scarless, ssODN-mediated editing. All sequence deviations from the expected knock-in (*Top*) and WT sequences (*Bottom*) within the span of the ssODN homology region are shown. Sequence highlighting is as in Figs. 1*C* and 2*C*. (*E*) Immunoblot analysis of the four scarless, sequenced mutants (labeled 1–4) shown in *C* and *D*.

Institute for Brain Research, Department of Brain and Cognitive Sciences, and Department of Biological Engineering, Massachusetts Institute of Technology, Cambridge, MA (plasmids 69982 and 69988, respectively; Addgene). The Cpf1 coding sequence and C-terminal nuclear localization signal were PCR-amplified to include 5′ SpeI and 3′ BsrGI sites and a C-terminal 6xHIS tag (Table S1). PCR fragments were cloned into plant transformation binary vector pK7FWG2 as SpeI-BsrGI fragments. GFP-targeting Cpf1 gRNA sequences were added downstream of the U6 promoter by PCR using pEN-Chimera (62) as template DNA (Table S1). Resultant PCR products were cloned as SmaI-EcoRV fragments into vector pB7WG. The GFP-targeting Cas9 gRNA sequence was annealed by using two single-stranded oligonucleotides and ligated into BbsI-linearized pEN-Chimera (Table S1). The customized RNA chimera was then transferred into Cas9-expressing plant transformation binary vector pDe-CAS9 by a single-site Gateway LR reaction (Invitrogen) as previously described (62).

***N. benthamiana* Growth Conditions.** GFP-expressing *N. benthamiana* line 16c (63) was grown under 100 μmol·m^{-2}·s^{-1} light in a 16-h photoperiod at 21 °C in Microclima cabinets (Snijders Labs).

Transient Gene Expression and Mutation Analysis in *N. benthamiana*. *Agrobacterium tumefaciens* strain AGL1 was transformed with Cpf1, Cas9, and GFP-targeting gRNA binary vectors and selected by using 100 μg/mL spectinomycin and 50 μg/mL rifampicin. For each construct, overnight starter cultures in lysogeny broth (LB) medium with antibiotics were used to inoculate 10 mL of medium for overnight incubation at 28 °C and 230 rpm (New Brunswick G25 Incubator Shaker). Overnight cultures were then centrifuged, resuspended in infiltration buffer (10 mM MES, pH 5.6, 300 μM acetosyringone, 10 mM $MgCl_2$), and incubated for 3 h at room temperature. Cells were adjusted to an OD_{595} of 1.0. AsCpf1 and LbCpf1 cultures were mixed 1:1 with their respective gRNA cultures. Accordingly, the Cas9 culture was adjusted to an OD_{595} of 0.5. For gRNA-only infiltrations, gRNA cultures were also adjusted to an OD_{595} of 0.5. Cells were infiltrated into the underside of 4–6-wk-old *N. benthamiana* line 16c leaves by using a 1-mL syringe without a needle. Infiltrated tissue was harvested at 3 d after infiltration. Leaf genomic DNA was extracted by using a GenElute Plant Genomic DNA MiniPrep Kit (Sigma) and used for PCR amplification of the *GFP* locus (Table S1). PCR products were twofold diluted into 1× NEBuffer 2 (New England Biolabs) and then denatured and reannealed for heteroduplex formation (95 °C, 10 min; 95–85 °C at −2 °C/s; 85–25 °C at −0.3 °C/s). Heteroduplexes were supplemented with T7 endonuclease (0.2 U/μL; New England Biolabs) and incubated at 37 °C for 1 h. DNA was resolved on a 2% agarose gel with SYBR Safe staining (Invitrogen) and imaged on a UVP BioDoc-It system.

In Vitro Synthesis and Purification of Cpf1 gRNAs. ssDNA oligonucleotides containing the reverse complement of the gRNA sequences were annealed in equimolar quantities to a short T7 RNA polymerase priming sequence in 1× T7 transcription buffer (Invitrogen; Table S1). In vitro transcription was performed in 100 μL reaction volumes containing annealed template DNA (0.1 μg/μL), RNAseOUT (1 U/μL; Invitrogen), 7.5 mM of each rNTP, 30 mM $MgCl_2$, 10 mM DTT, and T7 RNA polymerase (2 U/μL; Invitrogen) in 1× T7 transcription buffer (Invitrogen). Reactions were incubated at 37 °C overnight (16 h). After incubation, TURBO DNase was added to remove template DNA (0.2U/μL; Ambion) and incubated at 37 °C for 15 min; enzymes were then inhibited with EDTA (25 mM). RNA was separated and purified from 10% denaturing TBE-UREA polyacrylamide gels as previously described (64) and quantified using a NanoDrop 1000 spectrophotometer.

Purification of LbCpf1 Protein. *E. coli* codon-optimized LbCpf1 bearing an N-terminal MBP-TEV-HIS-NLS tag was a gift from Jin-Soo Kim, Center for Genome Engineering, Institute for Basic Science, Seoul, Republic of Korea and Department of Chemistry, Seoul National University, Seoul, Republic of Korea (plasmid 79008; Addgene). Rosetta (DE3) pLysS cells (EMD Millipore) were transformed with this vector and selected on 50 μg/mL carbenicillin and 50 μg/mL chloramphenicol. An overnight starter culture in LB medium with antibiotics was used to inoculate 1 L medium and incubated at 37 °C at 110 rpm (Panasonic MIR-S100-PE Orbital Shaker). When the culture reached an OD_{600} of 0.6, it was cooled to 16 °C for overnight induction (16 h) with isopropyl-β-D-thiogalactoside (IPTG, 0.5 mM). Cells were harvested and frozen at −80 °C until purification. Cells were resuspended in 10 mL extraction buffer 1 [50 mM Hepes, pH 7.5, 1 M NaCl, 5 mM $MgCl_2$, 1 mM PMSF, 10% glycerol, 1× EDTA-free Halt protease inhibitor (Thermo Scientific), 1 mg/mL lysozyme] and incubated on ice for 30 min. An equal volume of extraction buffer 2 was added [50 mM Hepes, pH 7.5, 1 M NaCl, 5 mM $MgCl_2$, 1 mM PMSF, 10% glycerol, 1× EDTA-free Halt protease inhibitor (Thermo Scientific), 20 mM imidazole, 4 mM β-mercaptoethanol, 500 mM γ-aminobutyric acid]. Cell lysate was sonicated by using a Soniprep 150 plus disintegrator and centrifuged (25,000 × *g*, 4 °C), and the supernatant was passed through a syringe filter (0.22 μm). Cobalt resin (HisPur; Thermo Scientific) was equilibrated in a gravity flow column (Econo-Pac; Bio-Rad) using equilibration buffer (50 mM Hepes, pH 7.5, 1 M NaCl, 5 mM $MgCl_2$, 10% glycerol, 10 mM imidazole, 250 mM γ-aminobutyric acid). Cell lysate was then applied, washed (50 mM Hepes, pH 7.5, 1 M NaCl, 5 mM $MgCl_2$, 10% glycerol, 10 mM imidazole, 2 mM β-mercaptoethanol, 250 mM γ-aminobutyric acid), and eluted (50 mM Hepes, pH 7.5, 1 M NaCl, 5 mM $MgCl_2$, 10% glycerol, 250 mM imidazole, 2 mM β-mercaptoethanol, 250 mM γ-aminobutyric acid). Elutions were analyzed by SDS/PAGE. LbCpf1-containing fractions were pooled and concentrated to 200 μL (Vivaspin 30k MWCO; GE Healthcare), and buffer was exchanged (Zeba 40k MWCO; Thermo Scientific) into storage buffer (20 mM Hepes, pH 7.5, 500 mM NaCl, 5 mM $MgCl_2$, 1% glycerol, 1 mM DTT, 250 mM γ-aminobutyric acid). Protein concentration was measured by using Bradford reagent (Sigma). Final concentration was 30 μg/μL. Single-use aliquots were snap-frozen in liquid nitrogen and stored at −80 °C.

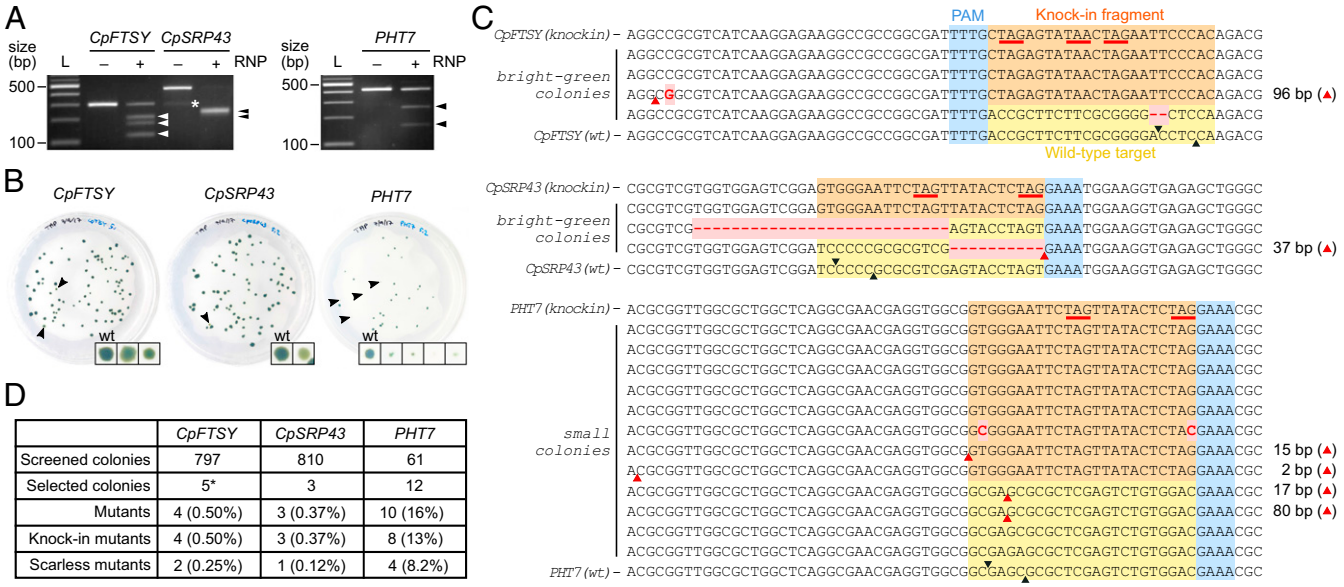

D

	CpFTSY	CpSRP43	PHT7
Screened colonies	797	810	61
Selected colonies	5*	3	12
Mutants	4 (0.50%)	3 (0.37%)	10 (16%)
Knock-in mutants	4 (0.50%)	3 (0.37%)	8 (13%)
Scarless mutants	2 (0.25%)	1 (0.12%)	4 (8.2%)

Fig. 4. Targeting of *CpFTSY*, *CpSRP43*, and *PHT7* using RNPs and sense ssODNs. (*A*) In vitro cleavage of *CpFTSY*, *CpSRP43*, and *PHT7*. Arrowheads indicate cleaved products, asterisk denotes a nonspecific band. L, ladder. (*B*) Representative plates of the bright-green phenotype of *CpFTSY* and *CpSRP43* mutants and the slow-growth phenotype of *PHT7* mutants (arrowheads). Indicated colonies are enlarged (*Bottom Right*) alongside a colony from each plate that was not identified through screening and is thus taken to represent WT. (*C*) Sequences from all cells identified as tentative *CpFTSY* (*Top*), *CpSRP43* (*Middle*), and *PHT7* (*Bottom*) mutants through phenotypic selection. Images of all screened plates and selected cells are in Figs. S5*B* and S6. All sequence deviations from the expected knock-in (*Top*) and WT sequences (*Bottom*) within the span of the ssODN homology region are shown. Sequence highlighting is as in Figs. 1*C*, 2*C*, and 3 *C* and *D*. (*D*) Numbers of screened colonies and sequence verified mutants identified in cells edited at *CpFTSY*, *CpSRP43*, and *PHT7*. Colony numbers as a proportion of all screened colonies are shown in parentheses. (*One tentative *CpFTSY* mutant grew as a mixed colony and could not be isolated; Fig. S6.)

In Vitro Cleavage Assay. Genomic DNA was extracted from *C. reinhardtii* by using a GenElute Plant Genomic DNA MiniPrep Kit (Sigma). Target loci were PCR-amplified and purified by using a MinElute PCR Purification Kit (Qiagen; Table S1). Purified LbCpf1 (200 nM) was preincubated with gRNA (600 nM) in cleavage buffer [1× NEBuffer 3 (New England Biolabs), 10 mM DTT, 10 mM $CaCl_2$] at 37 °C for 15 min. Target DNA (20 nM) was added to a final volume of 20 μL. Reactions were incubated at 37 °C for 1 h. Cleavage reactions were purified by using a MinElute PCR Purification Kit (Qiagen) and then resolved on 2% agarose gels with SYBR Safe staining (Invitrogen) and imaged on a UVP BioDoc-It system.

***C. reinhardtii* Cultures.** *C. reinhardtii* strains cc-1883 (*cw15*) and cc-2931 were provided by Sinead Collins, Ashworth Laboratories, School of Biology, University of Edinburgh, Edinburgh, UK. Cells were grown on Tris-acetate-phosphate (TAP) media (65) supplemented with 1% agar. Stock cultures were supplemented with 4 g/L yeast extract to encourage the growth of contaminants. Cells were grown under constant illumination with cool fluorescent white light (100 μmol photons·m^{-1}·s^{-1}) at 28 °C, and liquid TAP cultures were shaken at 110 rpm (Stuart SSL1 Orbital Shaker).

***Chlamydomonas* Transfection.** Cultures were grown to 2 × 10^6 cells per milliliter and counted by using a hemocytometer. For optional pretreatment of cc-2931, 5 × 10^5 cells were suspended and centrifuged (5 min, 1,500 × *g*) in Maxx Efficiency Transformation Reagent (1 mL) twice, followed by suspension in the same reagent supplemented with sucrose (40 mM). Purified LbCpf1 (100 μg, 0.526 nmol) was preincubated at a 1:3 molar ratio with gRNA (1.578 nmol) at 37 °C for 15 min to form RNP complexes. For transfection, 250 μL cell culture (5 × 10^5 cells) was supplemented with sucrose (40 mM) and mixed with preincubated RNPs. For template DNA-mediated editing, ssODN (5.26 nmol) was added at a 1:10 molar ratio to LbCpf1 (Table S1). Final volumes were 270–280 μL. Cells were electroporated in 4-mm cuvettes (600 V, 50 μF, 200 Ω) by using Gene Pulser Xcell (Bio-Rad) as suggested by Kwangryul Baek. Immediately after electroporation, 800 μL of TAP with 40 mM sucrose was added. Cells were recovered overnight (24 h) in 5 mL TAP with 40 mM sucrose shaken at 110 rpm (Stuart SSL1 Orbital Shaker) and then plated using 30% starch as previously described (20). Cells targeted at *FKB12* were plated onto TAP media supplemented with 10 μM rapamycin and grown under 20 μmol photons·m^{-1}·s^{-1} of constant illumination to limit rapamycin photodegradation. Cells targeted at *CpFTSY*, *CpSRP43*, and *PHT7* were plated onto regular TAP media and grown under 100 μmol photons·m^{-1}·s^{-1} of constant illumination. Cells targeted at *CpFTSY* and *CpSRP43* were screened for green coloration and chlorophyll fluorescence under a blue light transilluminator (Dark Reader; Clare Chemical Research). Cells targeted at *PHT7* were screened for small colonies at 7–9 d after plating. All plate images were taken by using a Canon camera (PowerShot G16) and were adjusted for brightness and contrast by using GIMP. Cells were counted by using OpenCFU (version 3.9.0) using default settings (66).

Sequence Analysis. *Chlamydomonas* colony PCR was performed by using Phire Plant Direct PCR Kit (Thermo Scientific) and appropriate primers (Table S1). To prepare reactions for sequencing, PCR reactions were twofold diluted, supplemented with exonuclease I (0.18 U/μL; New England Biolabs) and shrimp alkaline phosphatase (0.066 U/μL; New England Biolabs), and incubated at 30 °C for 30 min and then 80 °C for 10 min for enzyme denaturation. Reactions were sequenced by using BigDye Terminator version 3.1 (Applied Biosystems), followed by capillary analysis at Edinburgh Genomics. Low-quality sequences (typically Q40/length <0.3) were excluded together with mixed-read sequences. Sequences were aligned by using Clustal Omega (67).

Immunoblots. Liquid *C. reinhardtii* cell cultures were harvested and snap-frozen in midlog phase. Cells were suspended in extraction buffer (20 mM Tris·HCl, pH 7.5, 5 mM $MgCl_2$, 300 mM NaCl, 5 mM DTT, 0.1% Nonidet P-40, 1× EDTA-free Halt protease inhibitor; Thermo Scientific). Total soluble protein was extracted by two freeze/thaw cycles in liquid nitrogen followed by centrifugation at 17,000 × *g* for 15 min at 4 °C. The supernatant was measured using Bradford reagent (Sigma). Then, 40 μg total protein was resolved on a 16% Tricine SDS/PAGE gel (68). Running conditions were 30 V for 1 h followed by 50 V for 6 h. The gel was transferred onto a 0.45-μm nitrocellulose membrane by using the wet transfer method (30 V for 1 h at 4 °C). The membrane was blocked overnight with 5% milk and hybridized by using mouse anti-his antibodies [His-Tag (27E8) mouse mAb 2366; Cell Signaling Technology] and subsequently anti-mouse HRP-linked secondary antibodies (anti-mouse IgG, HRP-linked antibody 7076; Cell Signaling Technology). Peroxidase activity was detected by using Pierce ECL substrate (Thermo Scientific) and developed for 1 h.

ACKNOWLEDGMENTS. We thank Dr. Martin Wear, Dr. Sophie Kneeshaw, and Dr. Cihan Makbul for suggestions in protein purification, Kwangryul Baek for advising on *Chlamydomonas* electroporation, and Prof. Andrew Hudson for critically reading the manuscript. A.M. is a Chancellor's Fellow at the University of Edinburgh. This work was supported by the Biotechnology

and Biological Sciences Research Council (BBSRC) PHYCONET Proof of Concept Fund, Grant PHYCPoC-31. A.F. acknowledges support of BBSRC East of Scotland BioScience (EASTBIO) National Productivity Investment Fund (NPIF) Industrial Cooperative Awards in Science & Technology (CASE) studentship BB/R505493/1. D.E.P. was supported by BBSRC EASTBIO Grant BB/J01446X/1.

1. Harris EH (2001) *Chlamydomonas* as a model organism. *Annu Rev Plant Physiol Plant Mol Biol* 52:363–406.
2. Benning C (2015) Fueling research on *Chlamydomonas*. *Plant J* 82:363–364.
3. Goodenough U (2015) Historical perspective on *Chlamydomonas* as a model for basic research: 1950-1970. *Plant J* 82:365–369.
4. Wang Y, Duanmu D, Spalding MH (2011) Carbon dioxide concentrating mechanism in *Chlamydomonas reinhardtii*: Inorganic carbon transport and CO2 recapture. *Photosynth Res* 109:115–122.
5. Wang Y, Stessman DJ, Spalding MH (2015) The CO2 concentrating mechanism and photosynthetic carbon assimilation in limiting CO2 : How *Chlamydomonas* works against the gradient. *Plant J* 82:429–448.
6. Silflow CD, Lefebvre PA (2001) Assembly and motility of eukaryotic cilia and flagella. Lessons from *Chlamydomonas reinhardtii*. *Plant Physiol* 127:1500–1507.
7. Pazour GJ, Agrin N, Leszyk J, Witman GB (2005) Proteomic analysis of a eukaryotic cilium. *J Cell Biol* 170:103–113.
8. Pazour GJ, Agrin N, Walker BL, Witman GB (2006) Identification of predicted human outer dynein arm genes: Candidates for primary ciliary dyskinesia genes. *J Med Genet* 43:62–73.
9. Merchant SS, Kropat J, Liu B, Shaw J, Warakanont J (2012) TAG, you're it! Chlamydomonas as a reference organism for understanding algal triacylglycerol accumulation. *Curr Opin Biotechnol* 23:352–363.
10. Li-Beisson Y, Beisson F, Riekhof W (2015) Metabolism of acyl-lipids in *Chlamydomonas reinhardtii*. *Plant J* 82:504–522.
11. Scranton MA, Ostrand JT, Fields FJ, Mayfield SP (2015) *Chlamydomonas* as a model for biofuels and bio-products production. *Plant J* 82:523–531.
12. Lohr M, Im CS, Grossman AR (2005) Genome-based examination of chlorophyll and carotenoid biosynthesis in *Chlamydomonas reinhardtii*. *Plant Physiol* 138:490–515.
13. Philipps G, Happe T, Hemschemeier A (2012) Nitrogen deprivation results in photosynthetic hydrogen production in *Chlamydomonas reinhardtii*. *Planta* 235:729–745.
14. Boyle NR, et al. (2012) Three acyltransferases and nitrogen-responsive regulator are implicated in nitrogen starvation-induced triacylglycerol accumulation in *Chlamydomonas*. *J Biol Chem* 287:15811–15825.
15. Juergens MT, et al. (2015) The regulation of photosynthetic structure and function during nitrogen deprivation in *Chlamydomonas reinhardtii*. *Plant Physiol* 167: 558–573.
16. Maul JE, et al. (2002) The *Chlamydomonas reinhardtii* plastid chromosome: Islands of genes in a sea of repeats. *Plant Cell* 14:2659–2679.
17. Merchant SS, et al. (2007) The *Chlamydomonas* genome reveals the evolution of key animal and plant functions. *Science* 318:245–250.
18. Kindle KL, Schnell RA, Fernández E, Lefebvre PA (1989) Stable nuclear transformation of *Chlamydomonas* using the *Chlamydomonas* gene for nitrate reductase. *J Cell Biol* 109:2589–2601.
19. Kindle KL (1990) High-frequency nuclear transformation of *Chlamydomonas reinhardtii*. *Proc Natl Acad Sci USA* 87:1228–1232.
20. Shimogawara K, Fujiwara S, Grossman A, Usuda H (1998) High-efficiency transformation of *Chlamydomonas reinhardtii* by electroporation. *Genetics* 148: 1821–1828.
21. Kim S, et al. (2014) A simple and non-invasive method for nuclear transformation of intact-walled *Chlamydomonas reinhardtii*. *PLoS One* 9:e101018.
22. Harris EH, Stern DB, Witman GB (2009) *The Chlamydomonas Sourcebook* (Academic, San Diego), 2nd Ed.
23. Debuchy R, Purton S, Rochaix JD (1989) The argininosuccinate lyase gene of *Chlamydomonas reinhardtii*: An important tool for nuclear transformation and for correlating the genetic and molecular maps of the ARG7 locus. *EMBO J* 8:2803–2809.
24. Sodeinde OA, Kindle KL (1993) Homologous recombination in the nuclear genome of *Chlamydomonas reinhardtii*. *Proc Natl Acad Sci USA* 90:9199–9203.
25. Mayfield SP, Kindle KL (1990) Stable nuclear transformation of *Chlamydomonas reinhardtii* by using a *C. reinhardtii* gene as the selectable marker. *Proc Natl Acad Sci USA* 87:2087–2091.
26. Gumpel NJ, Rochaix JD, Purton S (1994) Studies on homologous recombination in the green alga *Chlamydomonas reinhardtii*. *Curr Genet* 26:438–442.
27. Slaninová M, Dominika H, Vlček D, Mages W (2008) Is it possible to improve homologous recombination in *Chlamydomonas reinhardtii*? *Biologia* 63:941–946.
28. Mages W, et al. (2007) Complementation of the *Chlamydomonas reinhardtii* arg7-8 (arg2) point mutation by recombination with a truncated nonfunctional ARG7 gene. *Protist* 158:435–446.
29. Zorin B, Hegemann P, Sizova I (2005) Nuclear-gene targeting by using single-stranded DNA avoids illegitimate DNA integration in *Chlamydomonas reinhardtii*. *Eukaryot Cell* 4:1264–1272.
30. Zorin B, Lu Y, Sizova I, Hegemann P (2009) Nuclear gene targeting in *Chlamydomonas* as exemplified by disruption of the PHOT gene. *Gene* 432:91–96.
31. Jiang WZ, Dumm S, Knuth ME, Sanders SL, Weeks DP (2017) Precise oligonucleotide-directed mutagenesis of the *Chlamydomonas reinhardtii* genome. *Plant Cell Rep* 36: 1001–1004.
32. Greiner A, et al. (2017) Targeting of photoreceptor genes in *Chlamydomonas reinhardtii* via zinc-finger nucleases and CRISPR/Cas9. *Plant Cell* 29:2498–2518.
33. Sizova I, Greiner A, Awasthi M, Kateriya S, Hegemann P (2013) Nuclear gene targeting in *Chlamydomonas* using engineered zinc-finger nucleases. *Plant J* 73:873–882.
34. Jiang W, Brueggeman AJ, Horken KM, Plucinak TM, Weeks DP (2014) Successful transient expression of Cas9 and single guide RNA genes in *Chlamydomonas reinhardtii*. *Eukaryot Cell* 13:1465–1469.
35. Shin SE, et al. (2016) CRISPR/Cas9-induced knockout and knock-in mutations in *Chlamydomonas reinhardtii*. *Sci Rep* 6:27810.
36. Baek K, et al. (2016) DNA-free two-gene knockout in *Chlamydomonas reinhardtii* via CRISPR-Cas9 ribonucleoproteins. *Sci Rep* 6:30620.
37. Bae S, Kweon J, Kim HS, Kim JS (2014) Microhomology-based choice of Cas9 nuclease target sites. *Nat Methods* 11:705–706.
38. van Overbeek M, et al. (2016) DNA repair profiling reveals nonrandom outcomes at Cas9-mediated breaks. *Mol Cell* 63:633–646.
39. Yoon HS, Hackett JD, Ciniglia C, Pinto G, Bhattacharya D (2004) A molecular timeline for the origin of photosynthetic eukaryotes. *Mol Biol Evol* 21:809–818.
40. Belhaj K, Chaparro-Garcia A, Kamoun S, Patron NJ, Nekrasov V (2015) Editing plant genomes with CRISPR/Cas9. *Curr Opin Biotechnol* 32:76–84.
41. Zetsche B, et al. (2017) Multiplex gene editing by CRISPR-Cpf1 using a single crRNA array. *Nat Biotechnol* 35:31–34.
42. Tu M, et al. (2017) A 'new lease of life': FnCpf1 possesses DNA cleavage activity for genome editing in human cells. *Nucleic Acids Res* 45:11295–11304.
43. Xu R, et al. (2017) Generation of targeted mutant rice using a CRISPR-Cpf1 system. *Plant Biotechnol J* 15:713–717.
44. Hu X, Wang C, Liu Q, Fu Y, Wang K (2017) Targeted mutagenesis in rice using CRISPR-Cpf1 system. *J Genet Genomics* 44:71–73.
45. Kim H, et al. (2017) CRISPR/Cpf1-mediated DNA-free plant genome editing. *Nat Commun* 8:14406.
46. Tang X, et al. (2017) A CRISPR-Cpf1 system for efficient genome editing and transcriptional repression in plants. *Nat Plants* 3:17018.
47. Crespo JL, Díaz-Troya S, Florencio FJ (2005) Inhibition of target of rapamycin signaling by rapamycin in the unicellular green alga *Chlamydomonas reinhardtii*. *Plant Physiol* 139:1736–1749.
48. Bae S, Park J, Kim JS (2014) Cas-OFFinder: A fast and versatile algorithm that searches for potential off-target sites of Cas9 RNA-guided endonucleases. *Bioinformatics* 30: 1473–1475.
49. Kirst H, García-Cerdán JG, Zurbriggen A, Melis A (2012) Assembly of the light-harvesting chlorophyll antenna in the green alga *Chlamydomonas reinhardtii* requires expression of the TLA2-CpFTSY gene. *Plant Physiol* 158:930–945.
50. Kirst H, Garcia-Cerdan JG, Zurbriggen A, Ruehle T, Melis A (2012) Truncated photosystem chlorophyll antenna size in the green microalga *Chlamydomonas reinhardtii* upon deletion of the TLA3-CpSRP43 gene. *Plant Physiol* 160:2251–2260.
51. Bothmer A, et al. (2017) Characterization of the interplay between DNA repair and CRISPR/Cas9-induced DNA lesions at an endogenous locus. *Nat Commun* 8:13905.
52. Richardson CD, et al. (2017) CRISPR-Cas9 genome editing in human cells works via the Fanconi anemia pathway. bioRxiv:10.1101/136028.
53. Zhang R, et al. (2014) High-throughput genotyping of green algal mutants reveals random distribution of mutagenic insertion sites and endonucleolytic cleavage of transforming DNA. *Plant Cell* 26:1398–1409.
54. Kim HK, et al. (2017) In vivo high-throughput profiling of CRISPR-Cpf1 activity. *Nat Methods* 14:153–159.
55. Doench JG, et al. (2014) Rational design of highly active sgRNAs for CRISPR-Cas9-mediated gene inactivation. *Nat Biotechnol* 32:1262–1267.
56. Chari R, Mali P, Moosburner M, Church GM (2015) Unraveling CRISPR-Cas9 genome engineering parameters via a library-on-library approach. *Nat Methods* 12:823–826.
57. Xu H, et al. (2015) Sequence determinants of improved CRISPR sgRNA design. *Genome Res* 25:1147–1157.
58. Doench JG, et al. (2016) Optimized sgRNA design to maximize activity and minimize off-target effects of CRISPR-Cas9. *Nat Biotechnol* 34:184–191.
59. Hough SH, Ajetunmobi A, Brody L, Humphryes-Kirilov N, Perello E (2016) Desktop genetics. *Per Med* 13:517–521.
60. Chen F, et al. (2017) Targeted activation of diverse CRISPR-Cas systems for mammalian genome editing via proximal CRISPR targeting. *Nat Commun* 8:14958.
61. Yamano T, Iguchi H, Fukuzawa H (2013) Rapid transformation of *Chlamydomonas reinhardtii* without cell-wall removal. *J Biosci Bioeng* 115:691–694.
62. Fauser F, Schiml S, Puchta H (2014) Both CRISPR/Cas-based nucleases and nickases can be used efficiently for genome engineering in *Arabidopsis thaliana*. *Plant J* 79: 348–359.
63. Ruiz MT, Voinnet O, Baulcombe DC (1998) Initiation and maintenance of virus-induced gene silencing. *Plant Cell* 10:937–946.
64. Harris CJ, Molnar A, Müller SY, Baulcombe DC (2015) FDF-PAGE: A powerful technique revealing previously undetected small RNAs sequestered by complementary transcripts. *Nucleic Acids Res* 43:7590–7599.
65. Gorman DS, Levine RP (1965) Cytochrome f and plastocyanin: Their sequence in the photosynthetic electron transport chain of *Chlamydomonas reinhardi*. *Proc Natl Acad Sci USA* 54:1665–1669.
66. Geissmann Q (2013) OpenCFU, a new free and open-source software to count cell colonies and other circular objects. *PLoS One* 8:e54072.
67. Li W, et al. (2015) The EMBL-EBI bioinformatics web and programmatic tools framework. *Nucleic Acids Res* 43:W580–W584.
68. Schägger H (2006) Tricine-SDS-PAGE. *Nat Protoc* 1:16–22.

Supporting Information

Ferenczi et al. 10.1073/pnas.1710597114

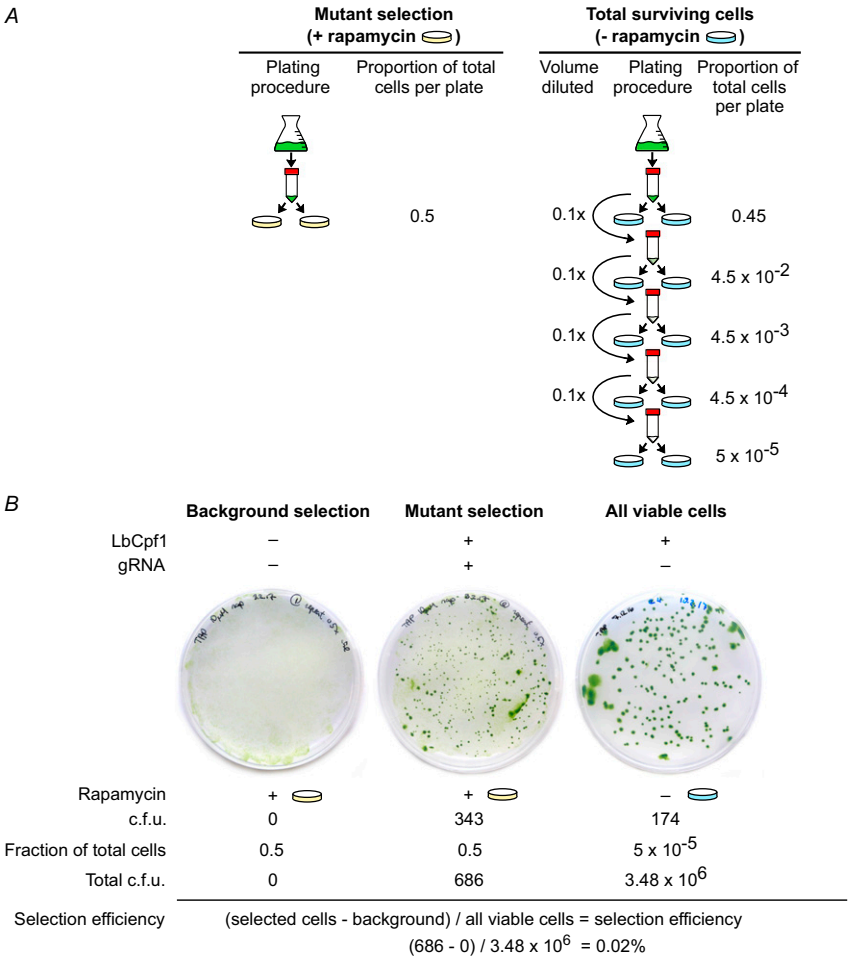

Fig. S1. Procedure to determine the proportion of rapamycin resistant cells through LbCpf1 RNP-mediated KO of the *FKB12* locus. (*A*) To obtain the number of *FKB12* mutants, cells transfected with LbCpf1 and gRNA RNPs were plated onto two solid growth media plates supplemented with 10 μM rapamycin. The same procedure was performed without RNPs to determine the background level of cell growth on rapamycin media. To determine all viable cells, we repeated the transfection omitting only the gRNA component and spread all cells onto two plates without rapamycin while using one tenth of the volume to perform serial dilutions. Each dilution was spread onto two plates. (*B*) Colony plates and counts (in cfu) for selected background cells (*Left*) and mutants (*Middle*). The rapamycin-resistant cells were sequence-verified for mutations in the *FKB12* locus (Fig. 1*C*). All viable cells were assessed by using a dilution containing a countable number of colonies (*Right*). Selection efficiency was counted as indicated.

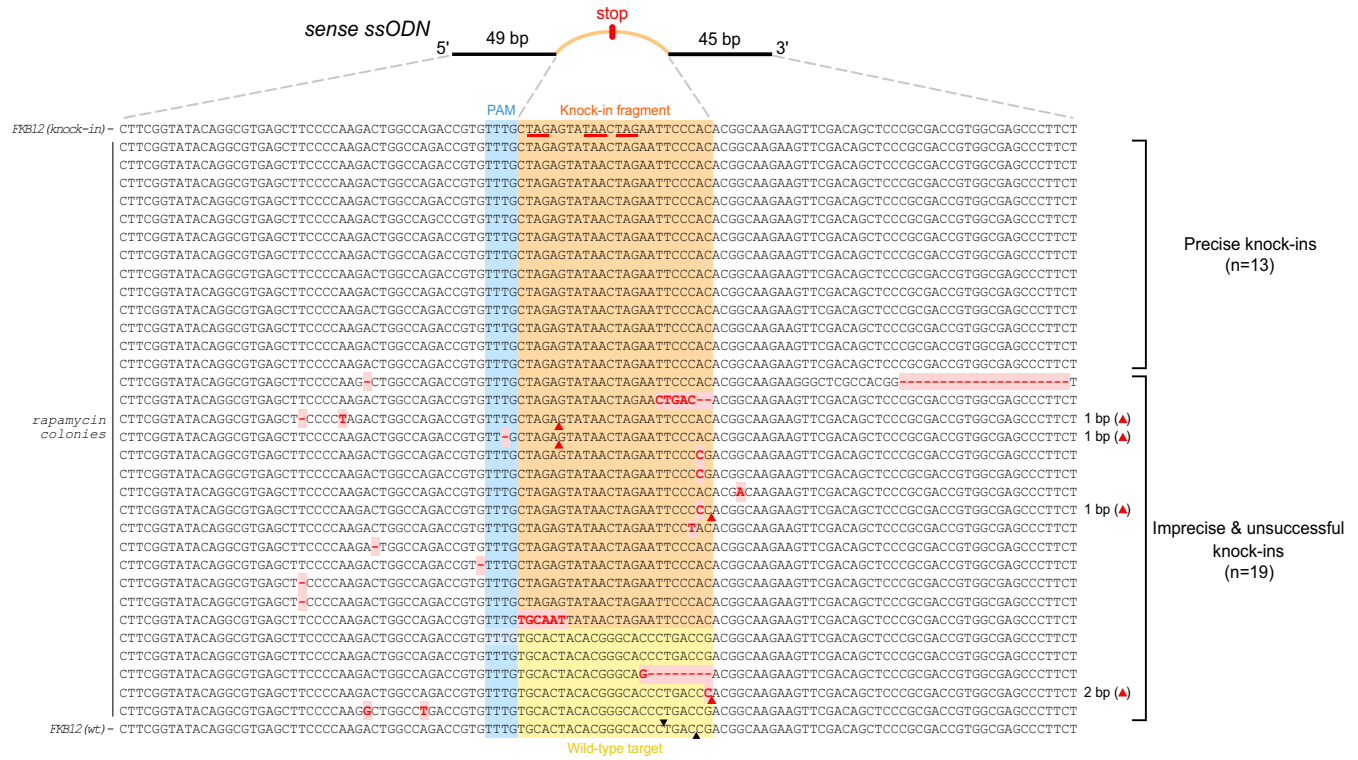

Fig. S2. All sequencing results of rapamycin-resistant cells cotransfected with RNPs and sense ssODN carrying three stop codons, one in each reading frame, targeting *FKB12* ($n = 32$). The entire span of ssODN homology is shown from the *FKB12* locus. Sequence highlighting is as in the figures in the main text.

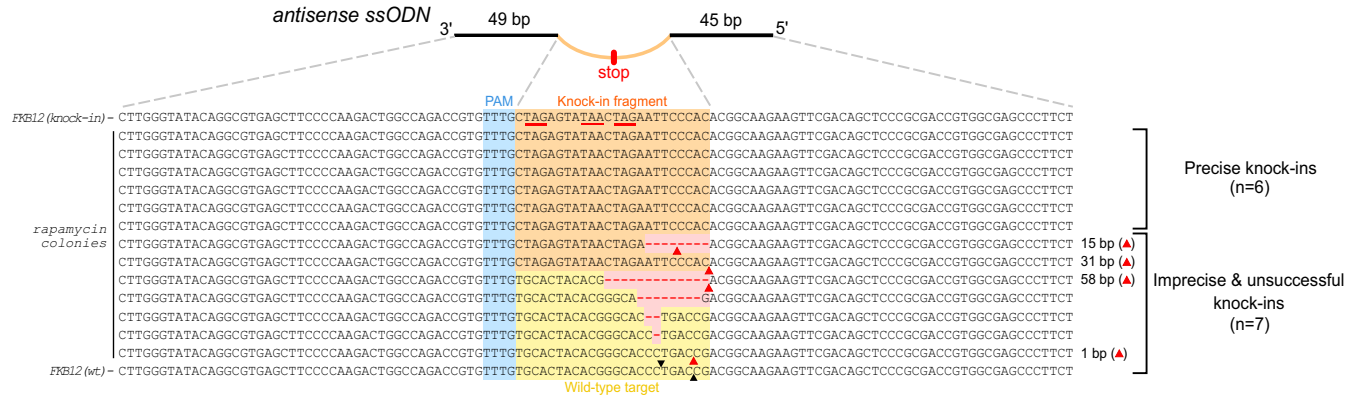

Fig. S3. All sequencing results of rapamycin-resistant cells cotransfected with RNPs and antisense ssODNs carrying three stop codons, one in each reading frame, targeting *FKB12* ($n = 13$). The entire span of ssODN homology is shown from the *FKB12* locus. Sequence highlighting is as in the figures in the main text.

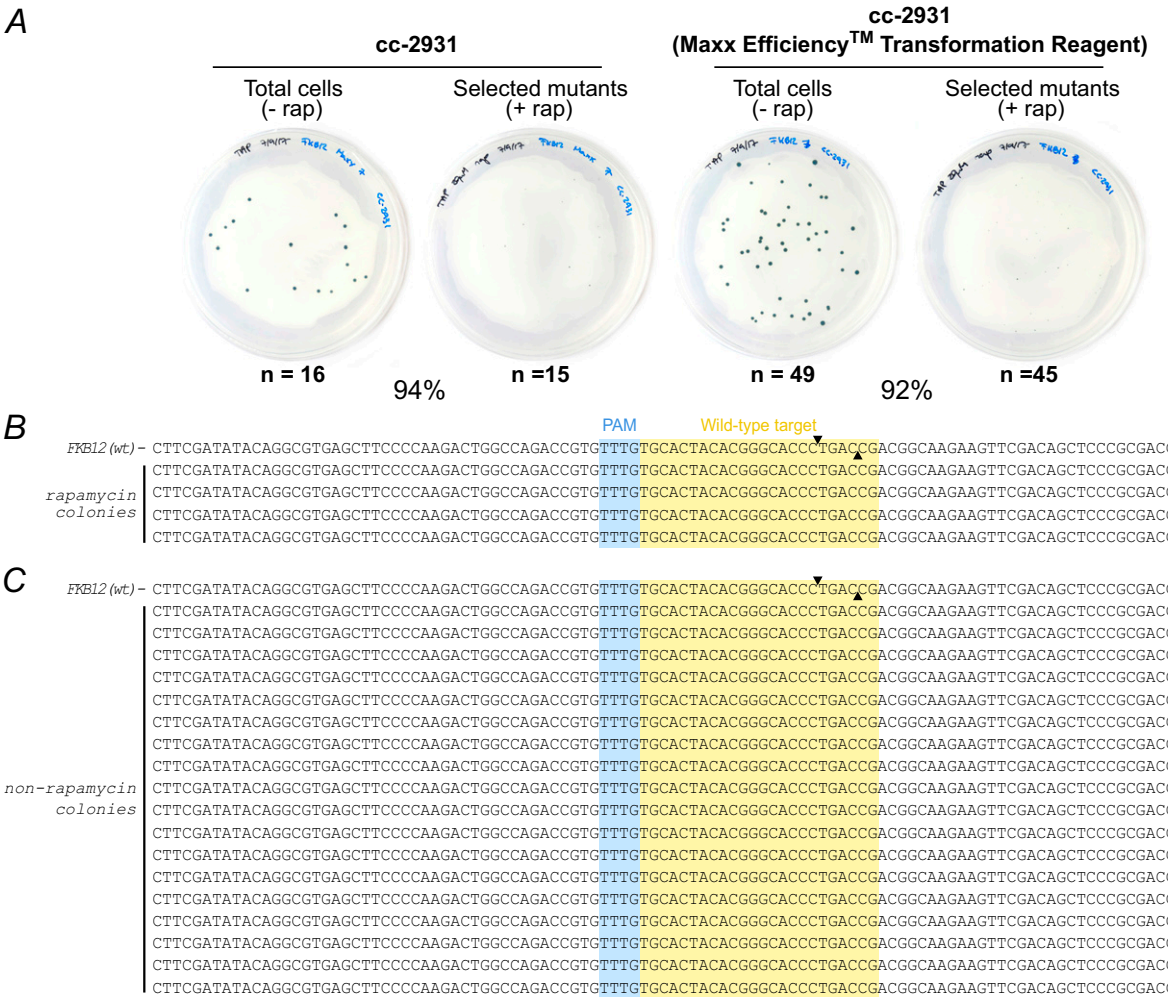

Fig. S4. RNP- and ssODN-mediated targeting at *FKB12* in cell-walled strain cc-2931. (*A*) Cells without (*Left*) and with (*Right*) Maxx Efficiency Transformation Reagent pretreatment followed by cotransfection with RNPs and sense ssODNs targeting *FKB12*. Cells were serially diluted and plated onto solid growth media with and without rapamycin (rap, 10 μM). A representative dilution is shown for both treatments. Note the small colony sizes on the rapamycin plates and almost identical numbers of colonies on plates with and without rapamycin selection, indicative of background growth rather than rapamycin-mediated selection of mutants. (*B*) *FKB12* sequences from small colonies from the rapamycin plate treated with Maxx Efficiency Transformation Reagent. (*C*) *FKB12* sequences of colonies from the nonrapamycin plate treated with Maxx Efficiency Transformation Reagent. Sequence highlighting is as in the figures in the main text.

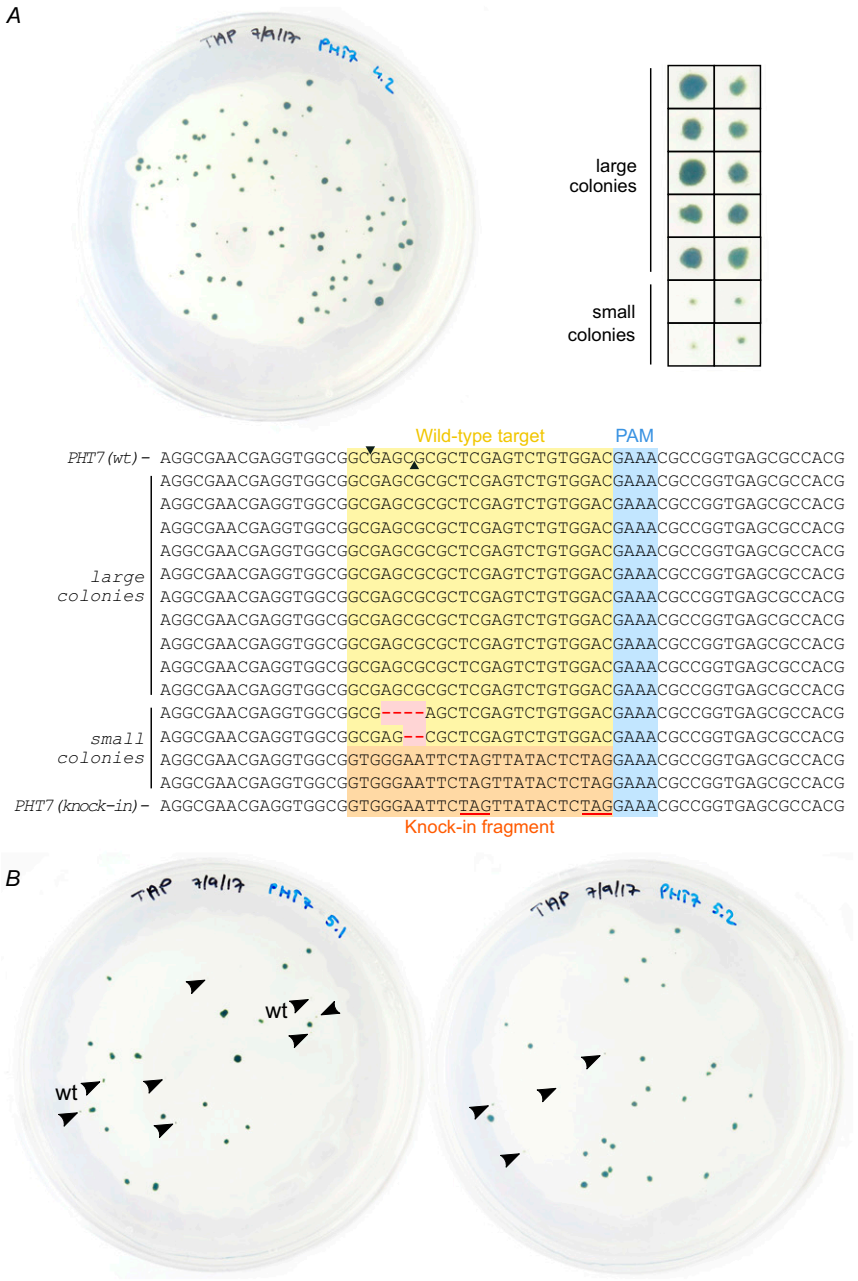

Fig. S5. Cells targeted for RNP- and ssODN-mediated gene editing at locus *PHT7*. (*A*) Preliminary sequencing of 14 colonies including four with a distinct small-colony phenotype. All small colonies were *PHT7* mutants. (*B*) Plates of cells targeted at *PHT7*, which were screened to determine editing efficiency. Colonies with a small-colony phenotype (arrowheads) were sequenced, revealing two WT colonies (wt). Sequencing of the indicated colonies is shown in Fig. 4*C*.

A

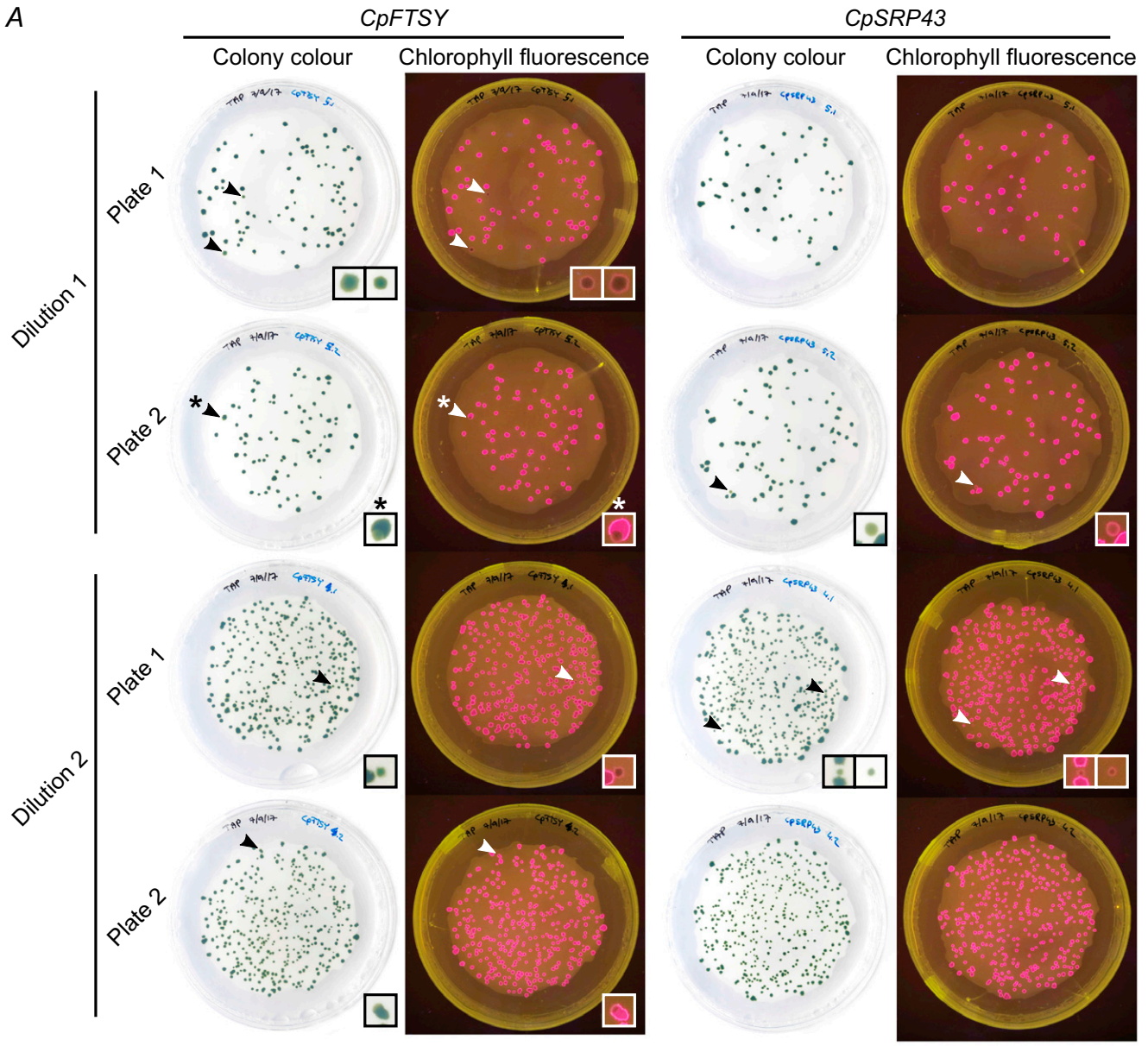

B

	CpFTSY					*CpSRP43*				
	Dilution 1		Dilution 2		Total	Dilution 1		Dilution 2		Total
	Plate 1	Plate 2	Plate 1	Plate 2		Plate 1	Plate 2	Plate 1	Plate 2	
All colonies	80	79	300	338	797	51	72	334	353	810
Bright green colonies	2	1	1	1	5	2	0	0	1	3

Fig. S6. Cells targeted with RNPs and ssODNs at *CpFTSY* and *CpSRP43*. (*A*) All plates of cell dilutions with colonies large and dispersed enough for phenotypic screening were examined for bright-green coloration under normal light and for chlorophyll fluorescence under a blue light transilluminator. Colonies identified through screening (arrowheads) are enlarged (*Bottom Right*). One mixed tentative *CpFTSY* mutant colony could not be isolated (asterisk). (*B*) Colony counts of all screened plates as shown in *A*.

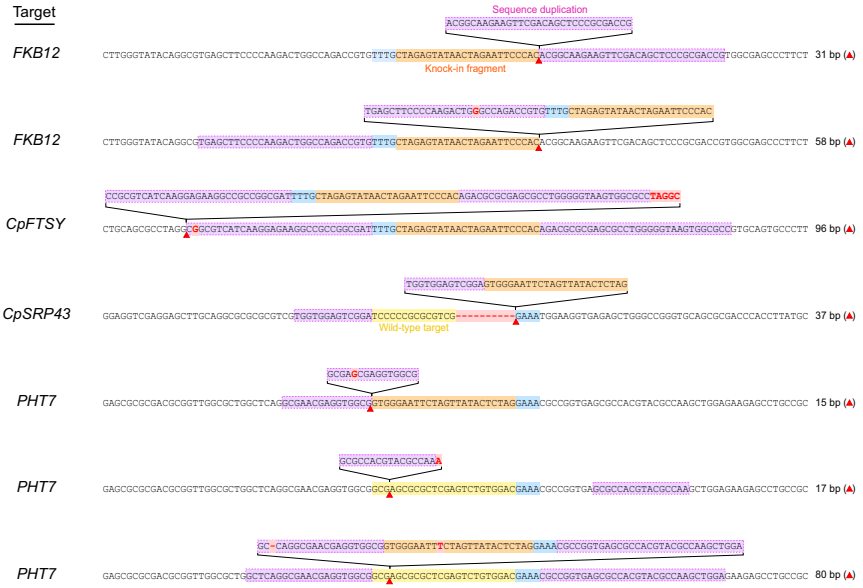

Fig. S7. Sequencing results of RNP and ssODN-mediated mutants that had partial ssODN duplications. Sequence duplications are indicted in purple with dashed outlines. Sequence highlighting is as in the figures in the main text.

Table S1. DNA material used in the study

Use	Forward primer/strand	Reverse primer/strand	PCR cycle
AsCpf1 amplification	TAACTAGTTGAATTCATGACACAGTTCGAGGGCTTT	AATGTACATTAGTGATGGTGATGGTGATGGGATCC-CTTTTTCTTTTTTGCCTGG	Q5 (NEB): 98 °C, 30 s > (98 °C, 10 s > 64 °C, 30 s > 72 °C, 2 min) × 35 > 72 °C, 2 min
LbCpf1 amplification	TAACTAGTTGAATTCATGAGCAAGCTGGAGAAGTTTACAA	AATGTACATTAGTGATGGTGATGGTGATGGGATCC-CTTTTTCTTTTTTGCCTGG	Q5 (NEB): 98 °C, 30 s > (98 °C, 10 s > 64 °C, 30 s > 72 °C, 2 min) × 35 > 72 °C, 2 min
PCR of U6 to make U6::GFP_gRNA for AsCpf1	TTTTTTCTTCTTCTTCGTTCATACAG	AAAAAACCGAGGATGTTTCCGTCCTCCTTATCTAC-AAGAGTAGAAATTACAAT-CACTACTTCGACTCTAGC	Q5 (NEB): 98 °C, 30 s > (98 °C, 10 s > 58 °C, 30 s > 72 °C, 15 s) × 35 > 72 °C, 2 min
PCR of U6 to make U6::GFP_gRNA for LbCpf1	TTTTTTCTTCTTCTTCGTTCATACAG	AAAAAACCGAGGATGTTTCCGTCCTCCTTATCTACA-CTTAGTAGAAATTACAATCACTACTTCGACTCTAGC	Q5 (NEB): 98 °C, 30 s > (98 °C, 10 s > 58 °C, 30 s > 72 °C, 15 s) × 35 > 72 °C, 2 min
GFP gRNA for Cas9	ATTGTAAGGGAATCGATTTCAAGG	AAACCCTTGAAATCGATTCCCTTA	Annealing cycle: 95 °C, 10 min; 95–85 °C at −2 °C/s; 85–25 °C at −0.3 °C/s
PCR of GFP locus from *N. benthamiana* 16c	AAACCCTTGAAATCGATTCCCTTA	ATATGAATTCTTAAAGCTCATCATGTTTGTATAGTTC	Taq (NEB): 96 °C, 30 s > (96 °C, 30 s > 62 °C, 30 s > 72 °C, 20 s) × 35 > 72 °C, 2 min
In vitro transcription of *FKB12* gRNA	GAAATTAATACGACTCACTATAGGG	CGGTCAGGGTGCCCGTGTAGTGCAATCTACACTTAGTA-GAAATTACCCTATAGTGAGTCGTATTAATTTC	Annealing cycle: 80 °C, 1 min > 80–20 °C at −0.3 °C/s
In vitro transcription of *CpFTSY* gRNA	GAAATTAATACGACTCACTATAGGG	TGGAGGTCCCCGCGAAGAAGCGGTATCTACACTTAGT-AGAAATTACCCTATAGTGAGTCGTATTAATTTC	Annealing cycle: 80 °C, 1 min > 80–20 °C at −0.3 °C/s
In vitro transcription of *CpSRP43* gRNA	GAAATTAATACGACTCACTATAGGG	TCCCCCGCGCGTCGAGTACCTAGTATCTACACTTA-GTAGAAATTACCCTATAGTGAGTCGTATTAATTTC	Annealing cycle: 80 °C, 1 min > 80–20 °C at −0.3 °C/s
In vitro transcription of *PHT7* gRNA	GAAATTAATACGACTCACTATAGGG	GCGAGCGCGCTCGAGTCTGTGGACATCTACACTT-AGTAGAAATTACCCTATAGTGAGTCGTATTAATTTC	Annealing cycle: 80 °C, 1 min > 80–20 °C at −0.3 °C/s
PCR of *FKB12* in cc-1883	CGTATCGGATGGGCAGCTTGAG	CGTCACTGTGTCCCAACGTGC	Taq (NEB): 96 °C, 2 min > (96 °C, 30 s > 62 °C, 30 s > 72 °C, 30 s)×35 > 72 °C, 10 min Phire (Thermo Fisher): 98 °C, 5 min > (98 °C, 5 s, 67 °C, 5 s, 72 °C, 10 s) × 40 > 72 °C, 1 min
PCR of *FKB12* in cc-2931	ATGGGTGTCGACGTCGCGACTA	GAAGTCGTGGCTGATGGTCAG	Phire (Thermo Fisher): 98 °C, 5 min > (98 °C, 5 s, 67 °C, 5 s, 72 °C, 10 s) × 40 > 72 °C, 1 min
PCR of *CpFTSY*	CTGCTTCAGACAGCCCTACC	GTGATTGGGTCGGCAAGTAC	Taq (NEB): 96 °C, 30 s > (96 °C, 30 s > 60 °C, 30 s > 72 °C, 20 s) × 35 > 72 °C, 2 min Phire (Thermo Fisher): 98 °C, 5 min > (98 °C, 5 s, 67 °C, 5 s, 72 °C, 10 s) × 40 > 72 °C, 1 min
PCR of *CpSRP43*	CTTATGCGAAAGCTGGCTTC	AAGTGCGGTGAAGAGTGCAG	Taq (NEB): 96 °C, 30 s > (96 °C, 30 s > 65 °C, 30 s > 72 °C, 20 s) × 35 > 72 °C, 2 min Phire (Thermo Fisher): 98 °C, 5 min > (98 °C, 5 s, 67 °C, 5 s, 72 °C, 10 s) × 40 > 72 °C, 1 min
PCR of *PHT7*, primer pair 1*	GTTCTTTGATGTCGGTGCCGTG	CTTGACAGCTAAGAGTACCCAACG	Taq (NEB): 96 °C, 30 s > (96 °C, 30 s > 65 °C, 30 s > 72 °C, 20 s) × 35 > 72 °C, 2 min Phire (Thermo Fisher): 98 °C, 5 min > (98 °C, 5 s, 67 °C, 5 s, 72 °C, 10 s) × 40 > 72 °C, 1 min
PCR of *PHT7*, primer pair 2	ACAGTCATGTGCACGGAATAGG	GACATCGATAACCCCTCCAGTC	Phire (Thermo Fisher): 98 °C, 5 min > (98 °C, 5 s, 67 °C, 5 s, 72 °C, 10 s) × 40 > 72 °C, 1 min
ssODN *FKB12* sense with stop codons (cc-1883)	CTTCGGTATACAGGCGTGAGCTTCCCCAA-GACTGGCCAGACCGTGTTTGCTAGAGTATA-ACTAGAATTCCCACACGGCAAGAAGTTCGA-CAGCTCCCGCGACCGTGGCGAGCCCTTCT	—	—

Table S1. Cont.

Use	Forward primer/strand	Reverse primer/strand	PCR cycle
ssODN *FKB12* antisense with stop codons	—	AGAAGGGCTCGCCACGGTCGCGGGAGCTGTCGAACTT- CTTGCCGTGTGGGAATTCTAGTTATACTCTAGCAAA- CACGGTCTGGCCAGTCTTGGGGAAGCTCACGCCTGTATACCGAAG	—
ssODN *FKB12* sense with stop codons (cc-2931)	CTTCGATATACAGGCGTGAGCTTCCCCAAGAC- TGGCCAGACCGTGTTTGCTAGAGTATAACTAG- AATTCCCACACGGCAAGAAGTTCGACAGCTC- CCGCGACCGTGGCGAGCCCTTCT	—	—
ssODN *FKB12* 6xHIS tag	CTTCGGTATACAGGCGTGAGCTTCCCCAAGAC- TGGCCAGACCGTGTTTCACCATCATCACCA- CCATTAAACCGACGGCAAGAAGTTCGACAG- CTCCCGCGACCGTGGCGAGCCCTTCT	—	—
ssODN *CpFTSY*	CTGCAGCGCCTAGGCCGCGTCATCAAGGA- GAAGGCCGCCGGCGATTTTGCTAGAGT- ATAACTAGAATTCCCACAGACGCGCGAG- CGCCTGGGGGTAAGTGGCGCCGTGCAGTGCCCTT	—	—
ssODN *CpSRP43*	GCATAAGGTGGGTCGCGCTGCACCCGGCCC- AGCTCTCACCTTCCATTTCCTAGAGTAT- AACTAGAATTCCCACTCCGACTCCACCAC- GACGCGCGCGCCTGCAAGCTCCTCGACCTCC	—	—
ssODN *PHT7*	GCGGCAGGCTCTTCTCCAGCTTGGCGTACGT- GGCGCTCACCGGCGTTTCCTAGAGTATAAC- TAGAATTCCCACCGCCACCTCGTTCGCCTGA- GCCAGCGCCAACCGCGTCGCGCGCTC	—	—

*This primer pair sometimes amplified nonspecific DNA fragments using Phire. For this purpose, we switched to *PHT7* primer pair 2.